Recent Progress of Double Quarkonium Production

Zhi-Guo He

College of Mathematics and Physics, Beijing University of Chemical Technology

15.03.2024, HAPOF-90, Beijing

Outline

1. Introduction
2. Review of double quarkonium hadroproduction
3. Relativistic effect in double J/ψ hadroproduction
4. Relativistic effect in double J/ψ photoproduction
5. Conclusion and summary

What is heavy quarkonium?

- Heavy quarkonium is one of the simplest QCD bound state constituted by heavy quark pair $Q\bar{Q}$ ($\Lambda_{QCD} \ll m_Q$).
- It is labeled by the spectroscopic notation $n^{2S+1}L_J$.
  - Its parity $P = (-1)^{L+1}$.
  - Its charge conjugation parity $C = (-1)^{L+S}$.
- There are 3 typical energy scales besides Λ_{QCD}:

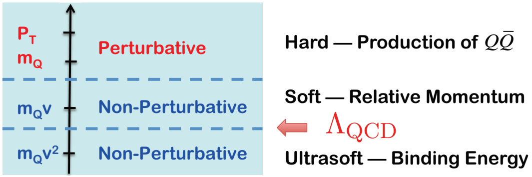

- It is an approximately non-relativistic system:
  - Charmonium: $v_c^2 \approx 0.23 \ll 1$
  - Bottomonium: $v_b^2 \approx 0.08 \ll 1$

Quarkonium production–The ideal laboratory to probe QCD

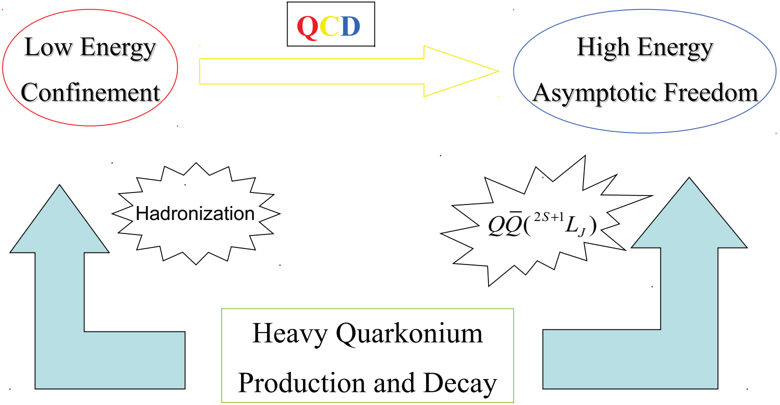

J/ψ and Υ are ideal candidates for their large leptonic branching functions!

Factorization of heavy quarkonium production

- The general factorization formalism:

$$\sigma_{(A+B\to quarkonium+X)} = \sum_n \int \sigma_{A+B\to(Q\bar{Q})_n+X} \times f[(Q\bar{Q})_n \to quarkonium]$$

- The models in market include color-singlet model (CSM), color evaporation model (CEM), and nonrelativistic QCD (NRQCD) factorization.

The challenges to NRQCD:

1. The long-standing J/ψ polarization puzzle.
2. The universality of the NRQCD LDMEs for J/ψ production up to QCD NLO.
3. The success of CSM to account for J/ψ production in e^+e^- annihilation, and η_c meson hadroproduction at the LHC.

Production mechanism of double quarkonium states

- Multi-final states can be produced through single parton scattering (SPS) or multi-parton scattering (MPS).

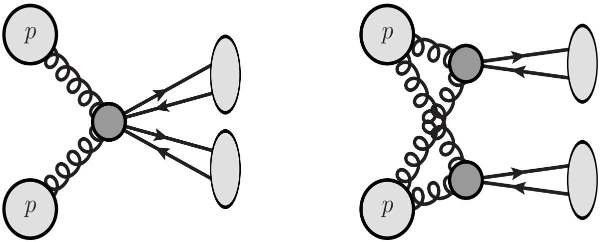

Schematical representation of SPS (left) and DPS (right) for a proton-proton collision. (Figure from Phys. Rev. D 95, 034029)

- The key parameter in MPS is σ_{eff}, which is supposed to be universal.

New features in quarkonium pair hadroproduction

1. Kinematically, it can be viewed as a gluon-gluon fusion type "Drell-Yan" process.
2. To test NRQCD factorization or other models, and to provide crucial constraint on the long-distance matrix elements. (Barger et al. 1996)
3. Help to improve the NRQCD factorization formalism for double P-wave production. (He et al. 2018)
4. To study the transverse momentum dependent parton distribution function. (Lansberg et al. 2018)
5. To extract σ_{eff} for DPS process. (Kom, et al. 2011)

Other benefits

- To help to understand the new fully heavy tetraquark states ($Q\bar{Q}Q\bar{Q}$). (LHCb Collaboration 2020)

Experimental Status of hadroproduction

Table: The summary experimental measurements

Experiment	$\sqrt{s}$	states	kinematic condition
D0	1.96 TeV	$J/\psi + J/\psi$	$p_T^{J/\psi} > 4.0\text{GeV}, \vert\eta^{J/\psi}\vert < 2$
		$J/\psi + \Upsilon$	$p_T^{\mu} > 2.0\text{GeV}, \vert\eta^{\mu}\vert < 2$
LHCb	7 TeV	$J/\psi + J/\psi$	$P_T^{J/\psi} < 10\text{GeV}\ 2.0 < y^{J/\psi} < 4.5$
	13 TeV	$J/\psi + J/\psi$	$P_T^{J/\psi} < 10(14)\text{GeV}$ $2.0 < y^{J/\psi} < 4.5$
		$J/\psi + \psi(2S)$	
CMS	7 TeV	$J/\psi + J/\psi$	$p_T^{J/\psi} > 4.5\text{GeV}, \vert y^{J/\psi}\vert < 2.2$
	8 TeV	$\Upsilon + \Upsilon$	$\vert y^{\Upsilon}\vert < 2.0$
	13 TeV		
ATLAS	8 TeV	$J/\psi + J/\psi$	$p_T^{J/\psi} > 8.5\text{GeV}, \vert y^{J/\psi}\vert < 2.1$

Rich observables

- σ, $\frac{d\sigma}{dp_T^{\psi}}$, $\frac{d\sigma}{dy^{\psi}}$, $\frac{d\sigma}{dp_T^{\psi\psi}}$, $\frac{d\sigma}{dy^{\psi\psi}}$, $\frac{d\sigma}{dm^{\psi\psi}}$, $\frac{d\sigma}{d|\Delta y|}$, $\frac{d\sigma}{d|\Delta \phi|}$ $\frac{d\sigma}{d\mathcal{A}_T}$.

Theoretical study of quarkonium pair hadroproduction I

Highlight of theoretical literature about SPS

- The J/ψ pair production was first proposed by Barger, et al. in 1996, in which the $2(c\bar{c}(^3S_1^{[8]}))$ contribution was studied.
- In 2002, Qiao found that the $2(c\bar{c}(^3S_1^{[1]}))$ channel contributes predominately to the total cross section.
- In 2009, Li et al. for the first time calculated the double η_c, and B_c hadroproduction.
- In 2011, it was suggested by Ko et al. that the $J/\psi + \Upsilon$ process may be a good probe of color octet (CO) mechanism.
- The higher order relativistic corrections to above subprocesses were calculated by Li, et al. in 2013.
- Baranov calculated the J/ψ pair production in $\mathrm{k_T}$ factorization approach in 2011, and in 2013 he and his collaborators considered the partial NNLO effect due to pseudodiffractive scattering.

Theoretical study of quarkonium pair hadroproduction II

To be continued

- The α_s^5 order real gluon emission effect was studied by Lansberg and Shao in 2013.
- The NLO QCD corrections to the $2(c\bar{c}(^3S_1^{[1]}))$ channel was obtained by Sun et al. in 2014.
- The complete LO NRQCD calculation including χ_c feed down were obtained by He and Kniehl in 2015.
- In 2016, the complete study of $J/\psi + \Upsilon$ production was carried out by Shao and Zhang.
- It was found by He et al. in 2018 that the NRQCD factorization breakdown when double P-wave states are involved.
- In 2019 He et al. studied the J/ψ pair production in the parton reggeization approach (PRA) with high-energy resummation.
- The NLO QCD corrections to $gg \to 2c\bar{c}(^1S_0^{[8]})$ channel was obtained by Sun in 2023.

Theoretical study of quarkonium pair hadroproduction III

Highlight of theoretical literature about DPS

- In 2011, Kom et al. were the first to realize that the J/ψ pair production is a good probe of the double parton scattering (DPS).
- Soon after, the DPS contribution to $J/\psi + \Upsilon$ was obtained by Baranov et al. for 7 TeV LHCb case with $\sigma_{\rm eff} = 14.5$ mb.
- $\sigma_{\rm eff} = 8.2 \pm 2.2$ mb was first extracted from J/ψ pair hadroproduction at CMS by Lansberg and shao in 2015.
- An upper bound of $\sigma_{\rm eff} < 8.2$ mb was gotten by Shao and Zhang from $J/\psi + \Upsilon$ production in 2016.
- A detailed study of DPS contribution to $2J/\psi$ production at LHC was performed by Borschensky and Kulesza in 2017 with $\sigma_{\rm eff} = 15$ mb.
- In 2020, $\sigma_{\rm eff} = 17.5 \pm 4.1$ mb and $\sigma_{\rm eff} = 13.8 \pm 0.9$ mb were determined by Prokhorov et al. from combined analysis of LHCb 7 and 13 TeV data.

σ_{eff} from experimental fit I

- In 2014, D0 Collaboration got $\sigma_{\text{eff}} = 4.8 \pm 0.5 \pm 2.5$ mb from double J/ψ hadroproduction. (left panel)
- Later in 2016 they got $\sigma_{\text{eff}} = 2.2 \pm 0.7 \pm 0.9$ mb from $J/\psi + \Upsilon$ hadroproduction. (right panel)

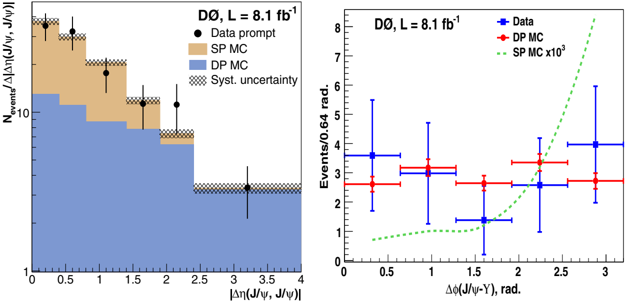

σ_{eff} from experimental fit II

- In 2017, ATLAS Collaboration got $\sigma_{\text{eff}} = 6.3 \pm 1.6 \pm 1.0$ mb from double J/ψ hadroproduction. (left panel)
- Later in 2023, the LHCb Collaboration got $\sigma_{\text{eff}} = 13.1 \pm 1.8 \pm 2.3$ mb from double J/ψ hadroproduction. (right panel)

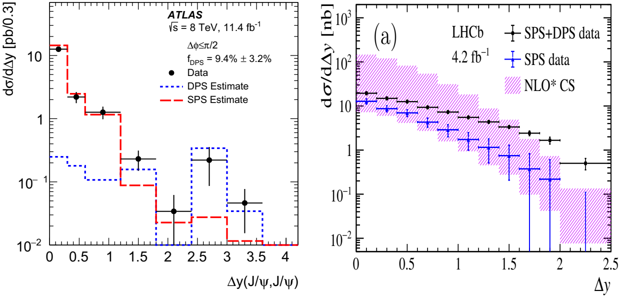

The experimental measurements are not consistent with each other too!

SPS contribution at LO

- Representative Feynman diagrams at LO:

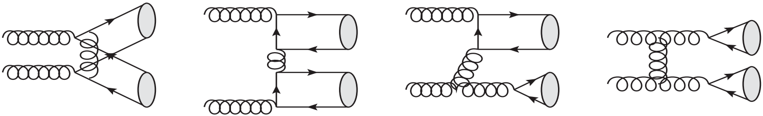

(a) (b) (c) (d)

According to the scaling $d\sigma/dp_T^2 \propto 1/p_T^N$ and the topological properties of the Feynman diagrams, sub-processes are divided into:

1. NNLP-I, with $N = 8$, including $m = {}^3S_1^{[1]}$ and $n = {}^3S_1^{[1,8]}, {}^1S_0^{[8]}, {}^3P_J^{[1,8]}$;
2. NNLP-II, with $N = 8$, too, including $m, n = {}^1S_0^{[8]}, {}^3P_J^{[1,8]}$;
3. NLP, with $N = 6$, including $m = {}^3S_1^{[8]}$ and $n = {}^1S_0^{[8]}, {}^3P_J^{[1,8]}$; and
4. LP, with $N = 4$, including $m = n = {}^3S_1^{[8]}$.

The p_t and v^2 behaviors for each channel

- Together with the velocity scaling rule of NRQCD LDMEs and assuming that the branch function is also of v^2 order, we can obtain the p_T and v^2 scaling of $d\sigma/dp_T^2$ for the relevant pairings (m, n) of $c\bar{c}$ Fock states of each $gg \to c\bar{c}(m)c\bar{c}(n)$ channel.

(m,n)	${}^3S_1^{[1]}$	${}^3S_1^{[8]}$	${}^1S_0^{[8]}$	${}^3P_J^{[8]}$	${}^3P_J^{[1]}$
${}^3S_1^{[1]}$	$1/p_T^8$	v^4/p_T^8	v^3/p_T^8	v^4/p_T^8	0
${}^3S_1^{[8]}$	—	v^8/p_T^4	v^7/p_T^6	v^8/p_T^6	v^8/p_T^6
${}^1S_0^{[8]}$	—	—	v^6/p_T^8	v^7/p_T^8	v^7/p_T^8
${}^3P_J^{[8]}$	—	—	—	v^8/p_T^8	v^8/p_T^8
${}^3P_J^{[1]}$	—	—	—	—	v^8/p_T^8

NRQCD predictions @ D0 1.96 TeV

- The fiducial cross sections reported by D0 Collaborations:

$$\sigma^{\rm SPS}_{\rm D0,fid} = (70 \pm 6 \pm 22)\ {\rm fb}, \sigma^{\rm DPS}_{\rm D0,fid} = (59 \pm 6 \pm 22)\ {\rm fb},$$

- The CSM predictions in LO (Qiao and Sun 2013) , $\rm k_T$ factorization (Baranov 2013) and $\rm NLO^*$ calculations (Lansberg and Shao 2013):

$$\sigma^{\rm SPS}_{\rm D0,fid} = 51.9\ {\rm fb}, \sigma^{\rm SPS,kT}_{\rm D0,fid} = 55.1^{+28.5\ +31.0}_{-15.6\ -17.0}\ {\rm fb}, \sigma^{\rm SPS,NLO^*}_{\rm D0,fid} = 90^{+180}_{-50}\ {\rm fb}.$$

- LO NRQCD predictions (He et al. 2021):

$$\sigma^{\rm SPS,NRQCD}_{\rm D0,fid} = 86.1^{+59.7}_{-34.0}\ {\rm fb},$$

The D0 conclusion depended on the SPS inputs. When complete NRQCD calculation is taken into account their conclusion might change.

NRQCD predictions @ LHCb 7 TeV

- Total cross section (nb): CSM predictions at QCD NLO (Sun eta al. 2016) and complete LO NRQCD (He, Kniehl 2015)

LHCb	LO CSM	NLO CSM	LO NRQCD
$5.1 \pm 1.0 \pm 1.1$	4.56 ± 1.13	$5.41^{+2.73}_{-1.14}$	$13.2^{+5.2}_{-4.1}$

- The invariant mass spectrum: NLO CSM, NRQCD LO, and $\mathrm{k_T}$(Baranov, Rezaeian 2016)

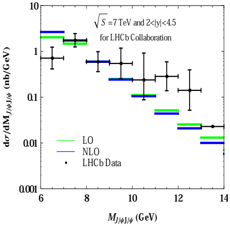

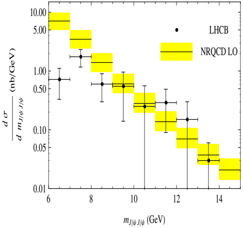

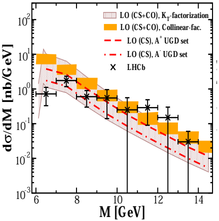

The theoretical predictions near threshold region strongly depend on the choice of m_c.

NRQCD predictions @ CMS 7 TeV I

- Total cross section (nb): NLO CSM (Sun eta al. 2023), complete LO NRQCD (He, Kniehl 2015), PRA (He et al. 2019)

CMS	LO CSM	NLO CSM	LO NRQCD	PRA
1.49 ± 0.07	0.048	0.18	$0.15^{+0.08}_{-0.05}$	$1.68^{+1.32}_{-0.78}$

- The J/ψ pair $\mathrm{p_T}$ distribution including prediction of $\mathrm{k_T}$ factorization (Baranov and Rezaeian 2016):

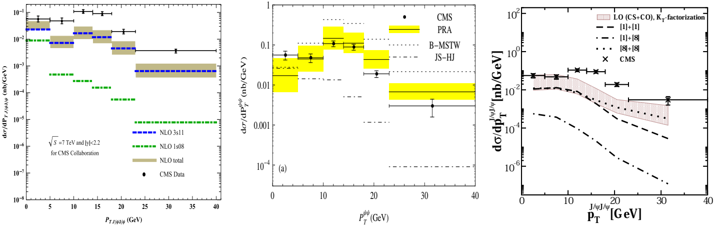

Different way of generating the $\mathrm{k_T}$ dependent PDF could lead to complete different predictions.

NRQCD predictions @ CMS 7 TeV II

- $|\Delta y|$ and $m_{\psi\psi}$ distributions: NLO CSM, LO NRQCD, k_T and PRA

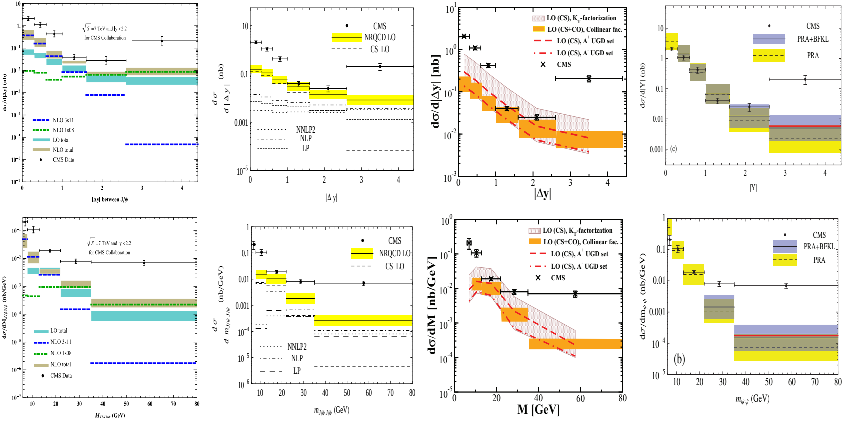

T-channel gluon exchange effect is significant and BKFL resummation can further enlarge fixed order calculations by a factor of 2.

NRQCD predictions @ ATLAS 8 TeV I

- Total cross section: PRA (He et al. 2019)

$$\sigma(pp \to J/\psi J/\psi + X) = \begin{cases} 82.2 \pm 8.3\,(\text{stat}) \pm 6.3\,(\text{syst}) \pm 0.9\,(\text{BF}) \pm 1.6\,(\text{lumi})\,\text{pb}, \text{ for } |y| < 1.05, \\ 78.3 \pm 9.2\,(\text{stat}) \pm 6.6\,(\text{syst}) \pm 0.9\,(\text{BF}) \pm 1.5\,(\text{lumi})\,\text{pb}, \text{ for } 1.05 \le |y| < 2.1. \end{cases}$$

$$\sigma^{\text{PRA}}_{\text{ATLAS}} = \begin{cases} 133.6^{+89.6}_{-52.2}\ \text{pb, for} |y(J/\psi_2)| < 1.05 \\ 105.2^{+73.8}_{-41.6}\ \text{pb, for} 1.05 < |y(J/\psi_2)| < 2.1 \end{cases}$$

- p_T distribution of single J/ψ

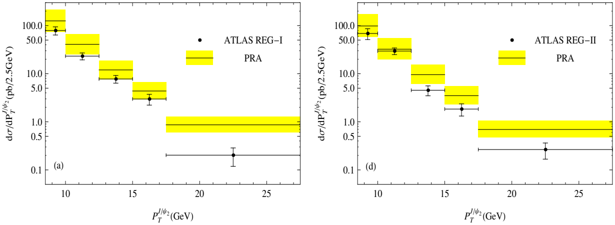

PRA predictions agree well with ATLAS measurements.

NRQCD predictions @ ATLAS 8 TeV II

- p_T and invariant mass distributions of the J/ψ pair:

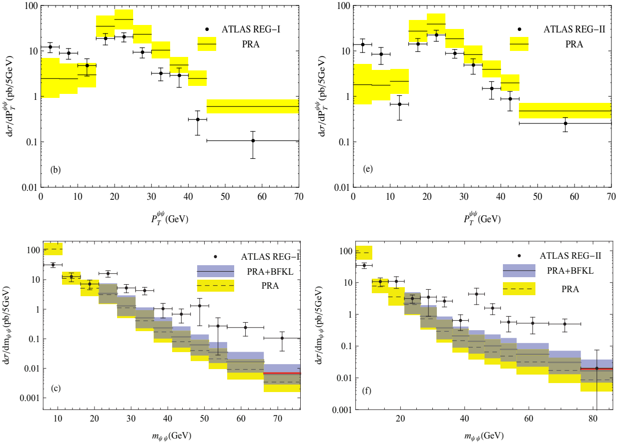

SPS can not account for the invariant mass distribution in the upper bins.

Why do we need the relativistic corrections?

- Theoretically, $v_c^2 \approx \alpha_s(2m_c)$ for charmonium.
- The NLO v^2 corrections played an important role to resolve the large discrepancy of double charmonium (He et al. 2007) and single J/ψ (He et al. 2010, Jia 2010) production in e^+e^-.
- For prompt J/ψ photo- and hadroproduction, the relativistic corrections have considerable influence on both yield and polarization. (He and Kniehl 2014,2015)
- In relativistic quark model calculation, the total cross sections of double J/ψ hadroproduction are significantly below LHCb measurements. (Martynenko and Trunin 2012)
- Previous investigation in NRQCD factorization found the relativistic corrections were tiny and depended strongly on the choice of m_c. (Li et al. 2013)

NRQCD factorization formalism up to v^2 NLO I

- Cross section in collinear parton model:

$$\sigma(A+B\to 2J/\psi+X)=$$
$$\sum_{i,j}\int \mathrm{d}x_1\mathrm{d}x_2 f_{i/A}(x_1)f_{j/B}(x_2)\hat{\sigma}(i+j\to 2J/\psi+X),$$

- The partonic cross section in NRQCD factorization up to v^2 order:

$$\hat{\sigma}(i+j\to 2J/\psi+X)=\sum_{m,n,H_1,H_2}\left(\frac{F^{ij}(m,n)}{m_c^{d_{\mathcal{O}(m)}-4}m_c^{d_{\mathcal{O}(n)}-4}}\right.$$
$$\times\langle\mathcal{O}^{H_1}(m)\rangle\langle\mathcal{O}^{H_2}(n)\rangle+\frac{G_1^{ij}(m,n)}{m_c^{d_{\mathcal{P}(m)}-4}m_c^{d_{\mathcal{O}(n)}-4}}\times\langle\mathcal{P}^{H_1}(m)\rangle\langle\mathcal{O}^{H_2}(n)\rangle$$
$$\left.+\frac{G_2^{ij}(m,n)}{m_c^{d_{\mathcal{O}(m)}-4}m_c^{d_{\mathcal{P}(n)}-4}}\times\langle\mathcal{O}^{H_1}(m)\rangle\langle\mathcal{P}^{H_2}(n)\rangle\right)$$
$$\times\mathrm{Br}(H_1\to J/\psi+X)\mathrm{Br}(H_2\to J/\psi+X)$$

NRQCD factorization formalism up to v^2 NLO II

- The definitions of S-wave 4-fermion operators in NRQCD:

$$\mathcal{O}^H({}^3S_1^{[1]}) = \chi^\dagger\sigma^i\psi(a_H^\dagger a_H)\psi^\dagger\sigma^i\chi,$$
$$\mathcal{P}^H({}^3S_1^{[1]}) = \chi^\dagger\sigma^i\psi(a_H^\dagger a_H)\psi^\dagger\sigma^i\left(-\frac{i}{2}\overleftrightarrow{\mathbf{D}}\right)^2\chi + \text{H.c.},$$

- Matching perturbative QCD and NRQCD calculations:

$$\hat{\sigma}(g+g\to(c\bar{c})_1+(c\bar{c})_2)\Big|_{\text{pert QCD}}$$
$$= \Big[\frac{F({}^3S_1^{[1]},{}^3S_1^{[1]})}{m_c^4}\langle 0|\mathcal{O}^{(c\bar{c})_1}({}^3S_1^{[1]})|0\rangle\langle 0|\mathcal{O}^{(c\bar{c})_2}({}^3S_1^{[1]})|0\rangle$$
$$+\frac{G_1({}^3S_1^{[1]},{}^3S_1^{[1]})}{m_c^6}\langle 0|\mathcal{P}^{(c\bar{c})_1}({}^3S_1^{[1]})|0\rangle\langle 0|\mathcal{O}^{(c\bar{c})_2}({}^3S_1^{[1]})|0\rangle$$
$$+\frac{G_2({}^3S_1^{[1]},{}^3S_1^{[1]})}{m_c^6}\langle 0|\mathcal{O}^{(c\bar{c})_1}({}^3S_1^{[1]})|0\rangle\langle 0|\mathcal{P}^{(c\bar{c})_2}({}^3S_1^{[1]})|0\rangle\Big]_{\text{pert NRQCD}}.$$

Spin projection method I

- Full QCD amplitude for double ${}^3S_1^{[1]}$ production:

$$\mathcal{M}\left(g+g\to(c\bar{c})_1({}^3S_1^{[1]})+(c\bar{c})_2({}^3S_1^{[1]})\right)=\sqrt{\frac{m_c}{E_{q_1}}}\sqrt{\frac{m_c}{E_{q_2}}}A(q_1,q_2),$$

where

$$\begin{aligned}A(q_1,q_2)=&\sum_{\lambda_i\bar{\lambda}_i k_i l_i}\langle\frac{1}{2},\lambda_1;\frac{1}{2},\bar{\lambda}_1|1,S_{1z}\rangle\langle 3,k_1;\bar{3},l_1|1\rangle\\ &\times\langle\frac{1}{2},\lambda_2;\frac{1}{2},\bar{\lambda}_2|1,S_{2z}\rangle\langle 3,k_2;\bar{3},l_2|1\rangle\\ &\times\mathcal{A}(g+g\to c_{\lambda_1,k_1}(p_{c_1})+\bar{c}_{\bar{\lambda}_1,l_1}(p_{\bar{c}_1})+c_{\lambda_2,k_2}(p_{c_2})+\bar{c}_{\bar{\lambda}_2,l_2}(p_{\bar{c}_2})),\end{aligned}$$

with $p_{c_i}=\frac{P_i}{2}+q_i$ and $p_{\bar{c}_i}=\frac{P_i}{2}-q_i$, and $E_{q_i}=\sqrt{m_c^2+\mathbf{q}^2}$.

Spin projection method II

- With the help of spin projection method, the matching can be implemented directly.
- The spin-triplet projector in arbitrary frame:

$$\sum_{\lambda_1,\bar{\lambda}_1} v(p_{\bar{c}},\bar{\lambda}_1)\bar{u}(p_c,\lambda_1)\langle\frac{1}{2},\lambda_1;\frac{1}{2},\bar{\lambda}_1|1,S_z\rangle =$$

$$\frac{1}{\sqrt{2}(E_q+m_c)}\times\left(\not{p}_{\bar{c}}-m_c\right)\not{\epsilon}\,\frac{\not{P}+2E_q}{4E_q}\left(\not{p}_c+m_c\right),$$

where ϵ^μ is the polarization vector, and the Dirac spinors are normalized as $\bar{u}u=-\bar{v}v=2m_c$

- The color projector of CS:

$$\langle 3,k_i;\bar{3},l_i|1\rangle = \frac{\delta_{k_i l_i}}{\sqrt{3}}$$

Expansion of squared amplitude – Explicit case

- Expansion the amplitude in series of q_1 and q_2:

$$
\begin{aligned}
A(q_1, q_2) =& A(0,0) + q_1^{\alpha_1} A_{\alpha_1,0} + q_2^{\beta_1} A_{0,\beta_1}(0,0) + \\
& \frac{1}{2} q_1^{\alpha_1} q_1^{\alpha_2} A_{\alpha_1\alpha_2,0}(0,0) + \frac{1}{2} q_2^{\beta_2} q_2^{\beta_2} A_{0,\beta_1\beta_2}(0,0) + \cdots .
\end{aligned}
$$

where

$$
A_{\alpha_1\cdots\alpha_m,\beta_1\cdots\beta_n}(0,0) \equiv \left. \frac{\partial^{m+n} A(q_1, q_2)}{\partial q_1^{\alpha_1} \cdots \partial q_1^{\alpha_m} \partial q_2^{\beta_1} \cdots \partial q_2^{\beta_n}} \right|_{q_1=0, q_2=0},
$$

- Decompose the higher rank tensor into S-wave:

$$
q^\mu q^\nu = \frac{|\mathbf{q}|^2}{3} \left(-g^{\mu\nu} + \frac{P\mu P^\nu}{4E_q^2} \right) = \frac{|\mathbf{q}|^2}{3} \Pi^{\mu\nu}
$$

Expansion of squared amplitude – Implicit case

- The $A(0,0)$ still depends on $\mathbf{q}_i^2$ implicitly through $P_i = 4E_{q_i}^2$ and the Mandelstam variables

$$t = (k_1 - P_1)^2 = (k_2 - P_2)^2, \quad u = (k_1 - P_2)^2 = (k_2 - P_1)^2,$$

- We introduce 2 new variables $\hat{t}$ and $\hat{u}$, and their non-relativistic limit:

$$\hat{t} \equiv t + \frac{s - 4E_{q_1}^2 - 4E_{q_2}^2}{2}, \quad \hat{u} \equiv u + \frac{s - 4E_{q_1}^2 - 4E_{q_2}^2}{2}$$

$$\hat{t}_0 \equiv t_0 + \frac{s - 8m_c^2}{2}, \quad \hat{u}_0 \equiv u_0 + \frac{s - 8m_c^2}{2}$$

- In the parton center of rest frame, t,u and t_0, u_0 are related through

$$\frac{\hat{t}}{\hat{t}_0} = \frac{\hat{u}}{\hat{u}_0} = \sqrt{\frac{\lambda(s, 4E_{q_1}^2, 4E_{q_2}^2)}{\lambda(s, 4m_c^2, 4m_c^2)}} \equiv k,$$

where

$$\lambda(a,b,c) = a^2 + b^2 + c^2 - 2ab - 2bc - 2ac.$$

Expansion of phase space

- The two-body phase space can be written in a simple form with $\hat{t}$ and $\hat{u}$, or with $\hat{t}_0$ and $\hat{u}_0$ as

$$\mathrm{d}\Phi_2 = \frac{\mathrm{d}\hat{t}\mathrm{d}\hat{u}}{8\pi s}\,\delta(\hat{t}+\hat{u}) = k\frac{\mathrm{d}\hat{t}_0\mathrm{d}\hat{u}_0}{8\pi s}\,\delta(\hat{t}_0+\hat{u}_0) = k\ \mathrm{d}\Phi_{20}.$$

where

$$k = \sqrt{1 - \frac{8\mathbf{q}_1^2 + 8\mathbf{q}_2^2}{s-16m_c^2} + \frac{16(\mathbf{q}_1^2 - \mathbf{q}_2^2)^2}{s(s-16m_c^2)}},$$

- All dependence on $\mathbf{q}_i^2$ are factorized into k, which makes the expansion of phase space become trivial.

Near threshold region, the expansion will be spoiled, for the actual expansion parameter is not $v^2 = \mathbf{q}^2/m_c^2$ anymore, but $8m_c^2 v^2/(s-16m_c^2)$.

"Rigorous" NRQCD results

- The formal results of matching:

$$\frac{F({}^3S_1^{[1]}, {}^3S_1^{[1]})}{m_c^4} = \frac{1}{2s}\int d\Phi_{20}|M|^2,$$

$$\frac{G^1({}^3S_1^{[1]}, {}^3S_1^{[1]})}{m_c^6} = \frac{G^2({}^3S_1^{[1]}, {}^3S_1^{[1]})}{m_c^6} = \frac{1}{2s}\int d\Phi_{20}(K|M|^2 + |N|^2).$$

where

$$|M|^2 = \overline{\sum}|A(0,0)|^2\Big|_{\mathbf{q}_{1,2}^2=0},$$

$$|N|^2 = \left\{\frac{\partial}{\partial \mathbf{q}_1^2}\left[\frac{m_c}{E_{q_1}}\overline{\sum}|A(0,0)|^2\right] + \frac{1}{3}\Pi_1^{\alpha_1\alpha_2}\mathrm{Re}\left[A^*(0,0)A_{\alpha_1\alpha_2,0}\right]\right\}\Big|_{\mathbf{q}_{1,2}^2=0}.$$

- Our results of $|N|^2$ agrees with literature except for a factor $1/2$ due to boson symmetry. The rigorous treatment of phase space is new.

Modified NRQCD calculation

- The physical mass of J/ψ and $\psi(2S)$ are used in phase space integral.
- m_c is preserved in matrix element calculation.
- $\hat{t}_0$ and $\hat{u}_0$ can be related to $\hat{t}_p$ and $\hat{u}_p$ in a similar way as:

$$\frac{\hat{t}_p}{\hat{t}_0} = \frac{\hat{u}_p}{\hat{u}_0} = \sqrt{\frac{\lambda(s, M_{H_1}^2, M_{H_2}^2)}{\lambda(s, 4m_c^2, 4m_c^2)}}$$

- In such a way, the theoretical uncertainties due to choice of m_c are largely reduced.

Note that in Li's paper, $m_c = M_{J/\psi}/2$, $m_c = (M_{J/\psi} + M_{\psi(2S)})/4$, and $m_c = M_{\psi(2S)}/2$ for 2 J/ψ, $J/\psi + \psi(2S)$ and 2 $\psi(2S)$,respectively.

Numerical inputs

- The LO LDMEs can be related to wave function in potential model calculation:

$$\mathcal{O}^{J/\psi}({}^3S_1^{[1]}) = 1.16\ \mathrm{GeV}^3, \mathcal{O}^{\psi(2S)}({}^3S_1^{[1]}) = 0.758\ \mathrm{GeV}^3.$$

- The ratios between LO and v^2 NLO LDMEs were calculated by Bodwin et al. in 2006,

$$\frac{\langle \mathcal{P}^{J/\psi}({}^3S_1^{[1]})\rangle}{\langle \mathcal{O}^{J/\psi}({}^3S_1^{[1]}\rangle} = 0.5\,\mathrm{GeV}^2 \simeq \frac{\langle \mathcal{P}^{\psi(2S)}({}^3S_1^{[1]})\rangle}{\langle \mathcal{O}^{\psi(2S)}({}^3S_1^{[1]})\rangle}.$$

- CTEQ6L1 LO pdf and one-Loop running of α_s with Λ^4=215 MeV.
- $\mu_r = \mu_f = \xi\left(\sqrt{4M_{H_1}^2 + p_T^2} + \sqrt{4M_{H_2}^2 + p_T^2}\right)/2$
- m_c =1.5GeV, $M_{J/\psi} = 3.097$GeV, $M_{\psi(2S)} = 3.686$GeV, and $\mathrm{Br}(\psi(2S) \to J/\psi + X) = 61.4\%$ are taken from PDG 2023.

NRQCD predictions @ v^2 NLO vs. LHCb 7 TeV data

- NLO v^2 corrections render 30% reduction to total cross section:

$$\sigma^{\rm Tot}_{\rm LHCb} = (5.1 \pm 1.0 \pm 1.1)\ {\rm nb},$$
$$\sigma^{\rm CS}_{\rm LO(v^2)} = 9.60^{+2.57}_{-2.73}\ {\rm nb},\ \sigma^{\rm CS}_{\rm NLO(v^2)} = 6.55^{+1.92}_{-1.89}\ {\rm nb}$$

- Invariant mass spectrum: The NLO v^2 contribution is -34% in direct production and -60% in $\psi(2S)$ feed-down, which lead to a total 45% reduction in the first bin.

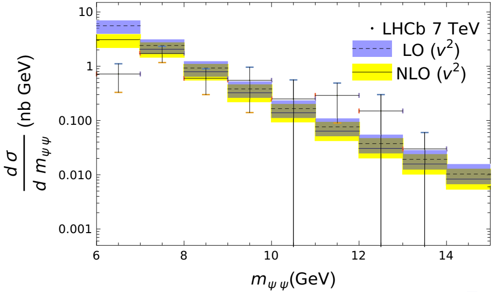

NRQCD predictions @ v^2 NLO vs. LHCb 13 TeV data I

- NLO total cross section: Conclusion similar to 7 TeV

$$\sigma^{\rm Tot}_{\rm LHCb} = (16.36 \pm 0.28 \pm 0.88)\ {\rm nb},\ \sigma^{\rm SPS}_{\rm LHCb} = (7.9 \pm 1.2 \pm 1.1)\ {\rm nb},$$
$$\sigma^{\rm CS}_{\rm LO(v^2)} = 17.43^{+2.44}_{-3.98}\ {\rm nb},\ \sigma^{\rm CS}_{\rm NLO(v^2)} = 12.02^{+1.98}_{-2.81}\ {\rm nb}$$

- Invariant mass spectrum: Compatible with experimental data except for the last bin leaving room for CO contribution.

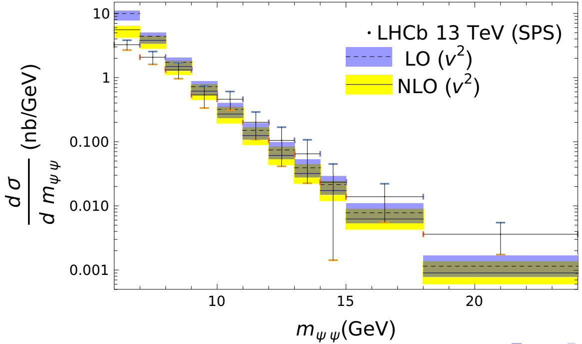

NRQCD predictions @ v^2 NLO vs. LHCb 13 TeV data II

- $y^{J/\psi}$ (left) and $|\Delta y|$ (right) spectrum: The NLO v^2 corrections make NRQCD predictions agree with LHCb measurements within errors.

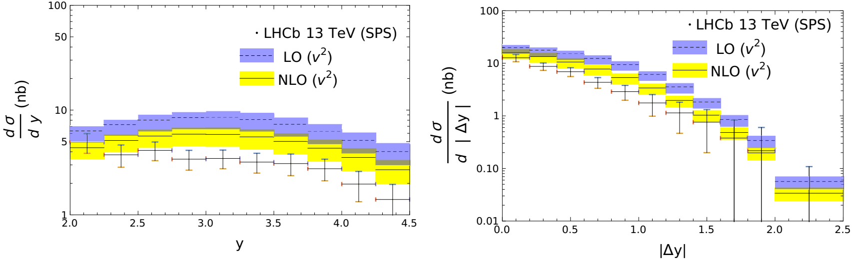

- The NLO v^2 corrections are constantly about -31% in all $y^{J/\psi}$ bins.
- The NLO v^2 corrections result in a reduction from 24% in the first bin to 40% in the last bin for $|\Delta y|$ distribution.

NRQCD predictions @ v^2 NLO vs. LHCb 13 TeV data III

- $J/\psi + \psi(2S)$ total cross section: LO predictions are reduced by 65%.

$$\sigma^{\rm Tot}_{\rm LHCb} = (4.49 \pm 0.71 \pm 0.26)\ \rm nb,$$
$$\sigma^{\rm CS}_{\rm LO(v^2)} = 16.23^{+2.17}_{-3.67}\ \rm nb,\ \sigma^{\rm CS}_{\rm NLO(v^2)} = 5.93^{+1.21}_{-1.44}\ \rm nb$$

- $m_{\psi\psi(2S)}$ (left) and $|\Delta y|$ (right) spectrum:

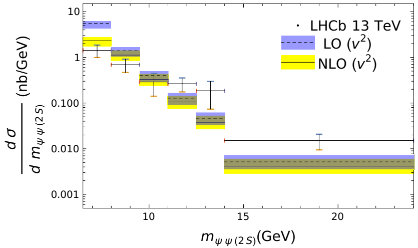

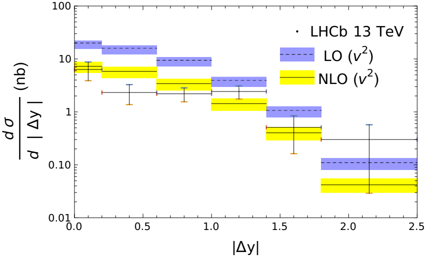

- All agree well with LHCb measurements except for large invariant mass region.

Modified vs. rigorous NLO v^2 corrections

- Comparison between modified and rigorous NRQCD predictions of invariant mass spectrum for direct 2 J/ψ production at 13 TeV LHCb.

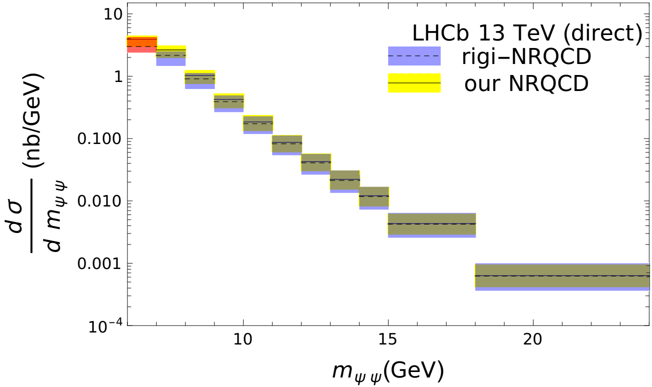

- In the first bin, the rigorous NRQCD prediction at v^2 NLO is negative!
- Their difference decreases dramatically as $m_{\psi\psi}$ increase.

Mode 1: $e^+e^- \to 2\gamma^* \to 2J/\psi$

- The LO process was introduced in 2002 by Bodwin et al..
- The NLO QCD corrections were obtained by Gong and Wang in 2008.
- The remarkable non-trivial NNLO QCD corrections were calculated very recently by 2 groups (Jia and Wang) in 2023.
- Representative Feynman diagrams up to QCD NNLO. (Huang et al. JHEP02 (2024) 055)

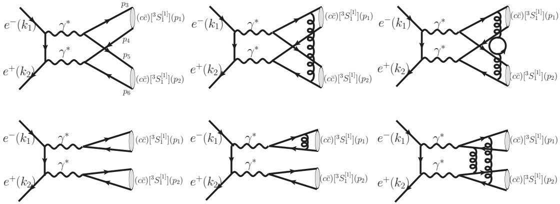

The total cross section drops down fast as $\sqrt{s}$ increase.

Mode 2: $e^+e^- \to Z \to 2J/\psi$

- The idea to study Z-boson contribution was raised by Chen et al. in 2013, and LO predictions were given.
- The NLO QCD corrections were considered by 2 groups (Berezhnoy et al. in 2021 and Luo et al. in 2022).
- Representative Feynman diagrams up to QCD NLO. (Luo et al. arXiv:2209.08802)

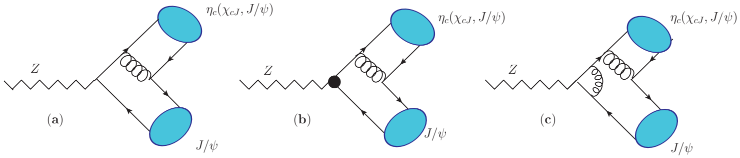

The cross section is tiny.

Mode 3: $\gamma\gamma \to 2J/\psi$

- The 2 J/ψ photoproduction was first considered by Qiao in 2002 as nonignorable contribution to single J/ψ photoproduction.
- The NLO QCD corrections were computed in 2020 by Yang et al..
- Representative Feynman diagrams up to QCD NLO. (Yang et al. Eur. Phys. J. C (2020) 80:806)

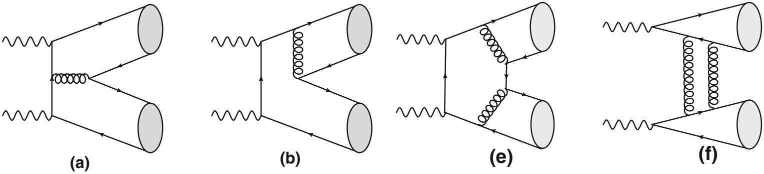

1. The production mechanism is relative simpler.
2. The NLO QCD corrections were large and negative.
3. The cross section is not small and increases as $\sqrt{s}$ becomes larger.

Prompt $2J/\psi$ photoproduction

- At high energy the quark or gluon content of photon can also participate in the hard collisions leading to 3 channels: Direct, Single-resolved, Double-resolved.
- The single-resolved channel played an important role to understand single J/ψ photoproduction at LEP. (Klasen 2002)
- The general formalism

$$\mathrm{d}\sigma(e^+e^- \to e^+e^- + 2J/\psi + X) =$$
$$\sum_{i,j,H_1,H_2} \int \mathrm{d}x_1 \mathrm{d}x_2 f_\gamma(x_1) f_\gamma(x_2) \int dx_i dx_j f_{i/\gamma}(x_i) f_{j/\gamma}(x_j) \times$$
$$\mathrm{d}\hat{\sigma}(i + j \to H_1 + H_2) \mathrm{Br}(H_1 \to J/\psi + X) \mathrm{Br}(H_2 \to J/\psi + X)\,,$$

where f_γ is the photon spectrum of $e^+(e^-)$, and $f_{i/\gamma}(x_i)$ is the PDF of parton i in the resolved photon.

Prompt $2J/\psi$ photoproduction

- We investigate 3 experiments: CEPC and FCC-ee at $\sqrt{s} = 92$ GeV, and CLIC at $\sqrt{s} = 3$TeV.
- We verified that both single and double resolved contributions are tiny up to $\sqrt{s} = 3$ TeV.
- In direct case, the CO channels are much suppressed by the NRQCD LDMEs.
- The CS channel includes:

$$\begin{aligned}\gamma + \gamma &\rightarrow (c\bar{c})_1({}^3S_1^{[1]}) + (c\bar{c})_2({}^3S_1^{[1]})\,,\\ \gamma + \gamma &\rightarrow (c\bar{c})_1({}^3P_{J_1}^{[1]}) + (c\bar{c})_2({}^3P_{J_2}^{[1]})\,.\end{aligned}$$

- It turns out that the SDCs of double P-wave cases are about one order of magnitude smaller.
- Further suppression factor of the branching functions.

The sources of photon and their spectra I

- At e^+e^- colliders, the photon can come from: (1)Bremsstrahlung, (2) Beamstrahlung, and (3) Laser back scattering.
- The Bremsstrahlung photon is described in WWA approximation:

$$f_\gamma^{WWA}(x) = \frac{\alpha}{2\pi}\left(\frac{1+(1-x)^2}{x}\log\left(\frac{Q^2_{\max}}{Q^2_{\min}}\right) + 2m_e^2 x\left(\frac{1}{Q^2_{\max}} - \frac{1}{Q^2_{\min}}\right)\right)$$

where $Q^2_{\min} = \frac{m_e^2 x^2}{1-x}$, $Q^2_{\max} = \left(\frac{\theta_c\sqrt{S}}{2}\right)^2(1-x) + Q^2_{\min}$.

- The spectrum of Beamstrahlung photon can be formulated as:

$$f_\gamma^{\rm beam}(x) = \frac{1}{\Gamma(\frac{1}{3})}\left(\frac{2}{3\Upsilon}\right)^{1/3} x^{-2/3}(1-x)^{-1/3}e^{-2x/(3\Upsilon(1-x))} \times$$
$$\left\{\frac{1-\sqrt{\Upsilon/24}}{g(x)}\left[1-\frac{1}{g(x)N_\gamma}\right](1-e^{-g(x)N_\gamma}) + \right.$$
$$\left.\sqrt{\frac{\Upsilon}{24}}\left[1-\frac{1}{N_\gamma}(1-e^{-N_\gamma})\right]\right\}$$

The sources of photon and their spectra II

- Υ is called effective beamstrahlung parameter, $N_\gamma = \frac{5\alpha\sigma_z m_e^2 \Upsilon}{2E_e\sqrt{1+\Upsilon^{2/3}}}$ is the averaged photon number emitted by e, and

$$g(x) = 1 - \frac{1}{2}\left((1+x)\sqrt{1+\Upsilon^{2/3}} + 1 - x\right)(1-x)^{2/3},$$

- The relevant parameters of CEPC,FCC-ee, and CLIC are:

Facility	collision energy	θ_c (mrad)	average Υ	bunch length σ_z(mm)	luminosity (ab^{-1}year^{-1})
FCC-ee	$\sqrt{s}$=92GeV	30	10^{-4}	15.5	17
CEPC	$\sqrt{s}$=92GeV	33	2×10^{-4}	8.7	15
CLIC	$\sqrt{s}$=3000GeV	20	5	0.044	0.6

- We calculate both NLO QCD and relativistic corrections.
- We choose $\mu_r = \sqrt{s}$, and require $p_T^{J/\psi} = 2$GeV, the other parameters are the same as hadroproduction.

NRQCD predictions at α_s and v^2 NLO – Cross section

- The total cross sections (fb) and number of lepton pair event produced per year:

	σ_{LO}	$\sigma_{\mathrm{NLO}}^{\alpha_s}$	$\sigma_{\mathrm{NLO}}^{v^2}$	$\sigma_{\mathrm{NLO}}^{\alpha_s,v^2}$	# of l^+l^-
FCC-ee	$5.88^{+2.99}_{-1.70}$	$3.21^{+0.18}_{-1.71}$	$5.17^{+2.64}_{-1.49}$	$2.65^{+0.34}_{-1.99}$	649^{+82}_{-488}
CEPC	$6.00^{+3.06}_{-1.73}$	$3.28^{+0.18}_{-1.75}$	$5.28^{+2.69}_{-1.53}$	$2.71^{+0.34}_{-2.03}$	584^{+75}_{-439}
CLIC	144^{+73}_{-36}	$78.9^{+3.9}_{-40.9}$	126^{+64}_{-32}	$64.6^{+7.5}_{-47.9}$	558^{+64}_{-414}

1. The Beamstrahlung contribution can be ignored in FCC-ee and CEPC cases, but enhance Bremsstrahlung predictions by about a factor of 2.6 at CLIC.
2. The v^2 corrections lead 12% reduction to LO predictions, and about $17^{+39}_{-6}\%$ on top of NLO QCD corrections.

NRQCD predictions at α_s and v^2 NLO – p_T distribution

- The $p_T^{J/\psi}$ distribution and number of lepton pair event produced per year in each bin:

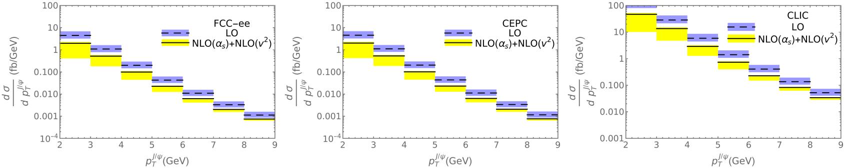

	1	2	3	4	5	6
FCC-ee	486^{+66}_{-386}	128^{+14}_{-83}	$24.4^{+2.3}_{-13.7}$	$5.6^{+0.4}_{-2.5}$	$1.5^{+0.1}_{-0.5}$	$0.5^{+0.0}_{-0.1}$
CEPC	438^{+59}_{-347}	115^{+13}_{-75}	$22.0^{+2.1}_{-12.3}$	$5.0^{+0.4}_{-2.3}$	$1.4^{+0.1}_{-0.5}$	$0.5^{+0.0}_{-0.1}$
CLIC	407^{+50}_{-319}	118^{+13}_{-77}	$25.2^{+2.4}_{-14.2}$	$6.4^{+0.5}_{-3.0}$	$2.0^{+0.1}_{-0.7}$	$0.7^{+0.0}_{-0.2}$

The $\alpha_s + v^2$ corrections lead to a reduction of $56^{+38}_{-27}\%$ in the fist bin down to $34^{+27}_{-21}\%$ in the last bin.

NRQCD predictions at α_s and v^2 NLO – y distribution

- The $y^{J/\psi}$ distribution and number of lepton pair event produced per year in each bin:

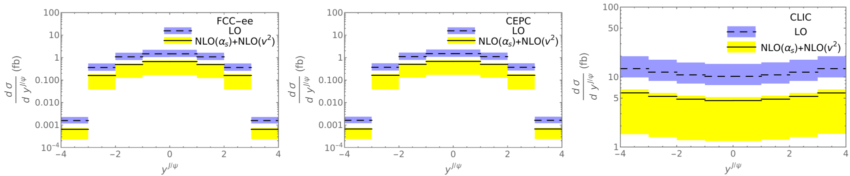

	1	2	3	4
FCC-ee	$0.16^{+0.0}_{-0.1}$	$39.4^{+5.3}_{-30.2}$	121^{+15}_{-90}	164^{+21}_{-123}
CEPC	$0.144^{+0.021}_{-0.093}$	$35.5^{+4.8}_{-27.2}$	109^{+14}_{-81}	147^{+19}_{-110}
CLIC	$51.5^{+6.2}_{-38.3}$	$45.9^{+5.5}_{-34.0}$	$41.9^{+5.0}_{-31.0}$	$39.9^{+4.8}_{-29.4}$

The $\alpha_s + v^2$ corrections lead to an almost uniformly reduction about $55^{+37}_{-26}\%$ except for the outermost bin.

NRQCD predictions at α_s and v^2 NLO – m_{jj} distribution

- The invariant mass distribution and number of lepton pair event produced per year in each bin:

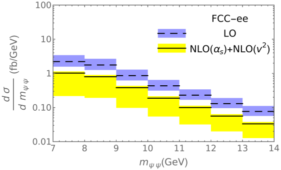

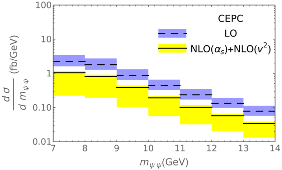

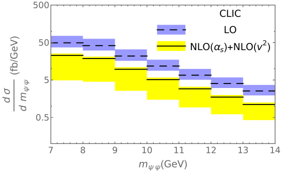

	1	2	3	4	5	6
FCC-ee	250^{+30}_{-197}	195^{+25}_{-148}	$93.5^{+12.4}_{-70.0}$	$46.1^{+6.5}_{-32.9}$	$24.4^{+3.4}_{-16.7}$	$13.8^{+1.9}_{-8.9}$
CEPC	225^{+27}_{-177}	176^{+23}_{-134}	$84.2^{+11.0}_{-62.3}$	$41.6^{+5.8}_{-29.6}$	$22.0^{+3.1}_{-15.0}$	$12.4^{+1.7}_{-8.1}$
CLIC	197^{+22}_{-154}	162^{+20}_{-123}	$83.8^{+10.7}_{-61.6}$	$44.4^{+5.8}_{-31.5}$	$25.2^{+3.3}_{-17.2}$	$15.1^{+2.0}_{-9.9}$

The reduction factor is the same as that in $y^{J/\psi}$ distribution.

Effect of NLO QCD or relativistic corrections

- The NLO QCD or relativistic corrections can be characterized by $k(\alpha_s) = d\sigma^{\mathrm{NLO}(\alpha_s)}/d\sigma^{\mathrm{LO}}$ and $k(v^2) = d\sigma^{\mathrm{NLO}(v^2,\alpha_s)}/d\sigma^{\mathrm{NLO}(\alpha_s)}$.
- For 3 experiment, the $k(\alpha_s)$, $k(v^2)$ are similar, we illustrate them in FCC-ee cases.

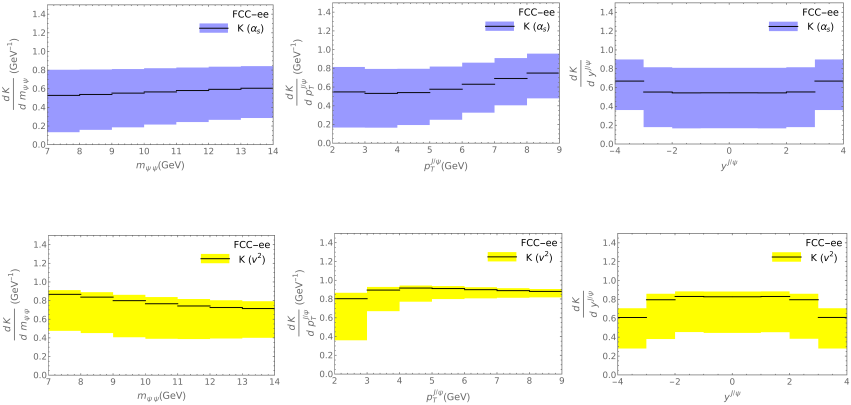

A few words about NLO QCD corrections

- Although the uncertainties due to μ variation still large, the band become narrow at QCD NLO.
- However, the predictions strongly depend on choice of the default μ.
- Differential cross sections of prompt double J/ψ photoproduction at FCC-ee with three different $\mu_r = \xi m_T$.

p_T (GeV)	$2-3$	$3-4$	$4-5$	$5-6$	$6-7$	$7-8$	$8-9$
$\mu_r = \sqrt{p_T^2 + 4m_c^2}/2$	-9.42	-1.90	-0.272	-0.0430	-0.00726	-0.00120	-0.000124
$\mu_r = \sqrt{p_T^2 + 4m_c^2}$	-0.162	0.0673	0.0270	0.00974	0.00370	0.00148	0.000620
$\mu_r = 2\sqrt{p_T^2 + 4m_c^2}$	1.81	0.519	0.0100	0.023	0.00647	0.00213	0.000790

The NLO QCD correction is negative and its absolute value increase as μ decrease that can even lead to un-physical prediction.

Conclusion and summary

1. Quarkonium pair hadroproduction can provide very rich probes to the perturbative and nonperturbative aspects of QCD as well as information about the partons inside proton.
2. Theoretically, their hadropoduction mechanism near threshold and in large invariant mass region is not yet understood.
3. The higher order relativistic corrections are important near the threshold region.
4. In prompt double J/ψ photoproduction, both the NLO QCD and relativistic corrections are negative.
5. There may be enough numbers of J/ψ that can be observed at FCC-ee, CEPC and CLIC.

Thank you!